



# **Development of Thin Films as Potential Structural Cathodes to Enable Multifunctional Energy-Storage Structural Composite Batteries for the U.S. Army's Future Force**

**by Eric Ngo, James Snyder, Clifford Hubbard, S. Garrett Hirsch, Conrad Xu,  
and Robert Carter**

**ARL-TR-5644**

**September 2011**

## **NOTICES**

### **Disclaimers**

The findings in this report are not to be construed as an official Department of the Army position unless so designated by other authorized documents.

Citation of manufacturer's or trade names does not constitute an official endorsement or approval of the use thereof.

Destroy this report when it is no longer needed. Do not return it to the originator.

# **Army Research Laboratory**

Aberdeen Proving Ground, MD 21005

---

**ARL-TR-5644****September 2011**

---

## **Development of Thin Films as Potential Structural Cathodes to Enable Multifunctional Energy-Storage Structural Composite Batteries for the U.S. Army's Future Force**

**Eric Ngo, James Snyder, Clifford Hubbard, S. Garrett Hirsch, Conrad Xu,  
and Robert Carter**

**Weapons Materials and Research Directorate, ARL**

REPORT DOCUMENTATION PAGE				Form Approved OMB No. 0704-0188	
<p>Public reporting burden for this collection of information is estimated to average 1 hour per response, including the time for reviewing instructions, searching existing data sources, gathering and maintaining the data needed, and completing and reviewing the collection information. Send comments regarding this burden estimate or any other aspect of this collection of information, including suggestions for reducing the burden, to Department of Defense, Washington Headquarters Services, Directorate for Information Operations and Reports (0704-0188), 1215 Jefferson Davis Highway, Suite 1204, Arlington, VA 22202-4302. Respondents should be aware that notwithstanding any other provision of law, no person shall be subject to any penalty for failing to comply with a collection of information if it does not display a currently valid OMB control number.</p> <p><b>PLEASE DO NOT RETURN YOUR FORM TO THE ABOVE ADDRESS.</b></p>					
1. REPORT DATE (DD-MM-YYYY)		2. REPORT TYPE		3. DATES COVERED (From - To)	
September 2011		FINAL		2009 to 2010	
4. TITLE AND SUBTITLE  Development of Thin Films as Potential Structural Cathodes to Enable Multifunctional Energy-Storage Structural Composite Batteries for the U.S. Army's Future Force				5a. CONTRACT NUMBER	
				5b. GRANT NUMBER	
				5c. PROGRAM ELEMENT NUMBER	
6. AUTHOR(S)  Eric Ngo, James Snyder, Clifford Hubbard, S. Garrett Hirsch, Conrad Xu, and Robert Carter				5d. PROJECT NUMBER	
				5e. TASK NUMBER	
				5f. WORK UNIT NUMBER	
7. PERFORMING ORGANIZATION NAME(S) AND ADDRESS(ES)  U.S. Army Research Laboratory ATTN: RDRL-WMM-E Aberdeen Proving Ground, MD 21005				8. PERFORMING ORGANIZATION REPORT NUMBER  ARL-TR-5644	
9. SPONSORING/MONITORING AGENCY NAME(S) AND ADDRESS(ES)				10. SPONSOR/MONITOR'S ACRONYM(S)	
				11. SPONSOR/MONITOR'S REPORT NUMBER(S)	
12. DISTRIBUTION/AVAILABILITY STATEMENT  Approved for public release; distribution unlimited.					
13. SUPPLEMENTARY NOTES					
14. ABSTRACT  Well formed films of pure $\text{LiMn}_2\text{O}_4$ were obtained by spin-coating stoichiometric amounts of manganese acetate $\text{Mn}(\text{CH}_3\text{COOH})_2 \cdot 4\text{H}_2\text{O}$ and lithium acetate $\text{Li}(\text{CH}_3\text{COOH})_2 \cdot 4\text{H}_2\text{O}$ dissolved in a mixture of acetic acid ( $\text{CH}_3\text{COOH}$ ) and 2-methoxyethanol ( $\text{H}_3\text{COCH}_2\text{CH}_2\text{OH}$ ) onto platinum coated silicon substrates. Several coats of solution were applied to reach the desired film thickness of approximately 200nm and then annealed at various temperatures ranging from 400 °C to 800 °C to crystallize the films into a spinel phase. The resulting films were characterized by scanning electron microscopy (SEM), X-ray diffraction (XRD), and atomic force microscopy (AFM). In addition, electrochemical properties were determined by cyclic voltammograms measurements. At 700 °C–800 °C, the films exhibited distinctly improved crystallinity and the spinel grains adopted a polyhedral shape of submicron size with well-defined edges and faces, thus enhancing particle connectivity. The films were found to deliver capacities around 0.12 mAh/cm <sup>2</sup> up to 25 cycles.					
15. SUBJECT TERMS  thin films, $\text{LiMn}_2\text{O}_4$ , metal organic solution deposition					
16. SECURITY CLASSIFICATION OF:			17. LIMITATION OF ABSTRACT  UU	18. NUMBER OF PAGES  18	19a. NAME OF RESPONSIBLE PERSON Eric Ngo
a. REPORT Unclassified	b. ABSTRACT Unclassified	c. THIS PAGE Unclassified			19b. TELEPHONE NUMBER (Include area code) (410) 306-0748

---

## Contents

---

<b>List of Figures</b>	<b>iv</b>
<b>1. Introduction</b>	<b>1</b>
<b>2. Experimental</b>	<b>1</b>
2.1 Base Materials .....	1
2.2 Process .....	1
2.3 Characterization.....	3
2.3.1 GAXRD .....	3
2.3.2 AFM .....	3
2.3.3 SEM.....	3
2.3.4 Electrochemical Measurements.....	3
<b>3. Results and Discussion</b>	<b>4</b>
<b>4. Conclusion</b>	<b>7</b>
<b>5. References</b>	<b>9</b>
<b>List of Symbols, Abbreviations, and Acronyms</b>	<b>10</b>
<b>Distribution List</b>	<b>11</b>

---

## List of Figures

---

Figure 1. MOSD processing scheme of $\text{LiMn}_2\text{O}_4$ .	2
Figure 2. XRD patterns of the as-deposited $\text{LiMn}_2\text{O}_4$ thin films on platinum silicon substrates at different annealing temperature (a) 400 °C; (b) 700 °C.	4
Figure 3. XRD patterns of the annealed $\text{LiMn}_2\text{O}_4$ thin films on platinum silicon substrates at 750 °C at various layers showing at 6 layers and above crystallinity were able to be obtained.	5
Figure 4. Atomic focus microscope shows the variation of the surface roughness and morphology with the annealing temperature (a) At 400 °C, the deposits exhibits earthworm-like morphology and (b) At 750 °C deposit exhibits dense and well-defined grains and earthworm-like vanished.	5
Figure 5. SEM and cross sectional of $\text{LiMn}_2\text{O}_4$ thin films on platinum silicon substrates at different annealing temperature (a) 400 °C and 45 degree cross section (b) 750 °C and 45 degree cross section.	6
Figure 6. (a) Charge and discharge data curves of 20 cycles illustrate electrochemical behavior of the 6 layers film annealed at 750C. (b) Voltage profile over 60 hours of $\text{LiMn}_2\text{O}_4$ films versus time.	7

---

## 1. Introduction

---

Recently, there has been a significant increase in the need for enhanced materials for multifunctional power-generation and energy-storage applications. The progress in the power industries has resulted in a demand for compact, high-energy, and multifunctional components, which are the keys for large power and integratable multifunctional batteries (1–5). Today, the lithium ion battery is widely used because of its ideal charge/discharge capability. Nevertheless, in order to meet the critical system-level reductions in mass and volume, a paradigm shift in the current battery technology must be developed via multifunctional components that simultaneously offer power generation/energy storage and the ability to bear significant structural loads. This interest has promoted extensive research into the materials and fabrication science of thin-film based micro-batteries and structural batteries (4, 5). Spinel lithium manganese oxide ( $\text{LiMn}_2\text{O}_4$ ) is an attractive cathode material for Li/Li<sup>+</sup> rechargeable batteries and has been extensively considered due to its high voltage, low cost, non-toxicity and high theoretical capacity (6, 7). In this report,  $\text{LiMn}_2\text{O}_4$  was processed in thin film form via metal organic solution deposition on platinum coated silicon substrates (Pt-Si) and then annealed at various temperatures from 400 °C to 800 °C to produce crystalline films. The structure, surface morphology, and charge/discharge performance of the  $\text{LiMn}_2\text{O}_4$  films were characterized by glancing angle X-ray diffraction (GAXRD), atomic force microscopy (AFM), scanning electron microscopy (SEM), and electrochemical cycling.

---

## 2. Experimental

---

### 2.1 Base Materials

All materials and chemicals were obtained from Alfa Aesar. The base materials used were manganese acetate ( $\text{Mn}[\text{CH}_3\text{COOH}]_2 \cdot 4\text{H}_2\text{O}$ ) (stock # 12982), lithium acetate ( $\text{Li}[\text{CH}_3\text{COOH}]_2 \cdot 4\text{H}_2\text{O}$ ) (stock # 10802), 2-methoxyethanol ( $\text{H}_3\text{COCH}_2\text{CH}_2\text{OH}$ ), and acetic acid ( $\text{CH}_3\text{COOH}$ ).

### 2.2 Process

$\text{LiMn}_2\text{O}_4$  thin films were obtained by a metal organic solution deposition (MOSD) spin-coating technique (8, 9). Figure 1 shows the general fabrication steps. Stoichiometric amounts of manganese acetate and lithium acetate were individually prepared and dissolved in 2-methoxyethanol. Acetic acid was then added to prevent rapid hydrolysis and precipitation of the metal oxide. The viscosity and surface tension of the solution was adjusted by varying the 2-methoxyethanol content. This step is necessary to ensure integrity and to allow the solution to adhere to the substrate. The precursor films were coated onto various substrates by spin-coating

at 3500 revolutions per minute (rpm) for 30 s using a Headway Research (Model A4700) photo-resist spinner. Each layer of deposition was heat treated between coats at 350 °C. This process was repeated for each coat, with multiple coats needed to achieve a desired thickness of 200–250 nm. A 0.2 micron syringe filter was used to remove dust and other suspended impurities and enhance the quality of the films. The thickness of the film was about 30 nm per coat and can be controlled by adjusting the viscosity of the solution and spin speed. The films were coated on Si, MgO and Pt-Si substrates depending on the measurement requirements (Si and MgO substrates for structural analysis, Pt-Si substrates for electrochemical measurement). Prior to film deposition, all the Si substrates were cleaned by a room-temperature spin etching using 2-methoxyethoxide and further treated by using atmospheric ultra violet (UV) plasma treatment to remove the native silicon oxide and create hydrogen terminated substrate surface in order to enhance reproducibility and consistency of the films. After spinning each layer of solution onto various substrates, the films were heated on a hot plate at 350 °C in air for 60 min to remove the solvents and organic components. This step was repeated after each coating to ensure complete removal of volatile matter. Once the last layer was deposited, the whole film coat was then heat treated for 1 hour at 450 °C. In the as-deposited condition, the films are amorphous and require additional annealing for crystallization. Annealing of the films was carried out in a Varian tube furnace at various temperatures, ranging from 400 °C to 800 °C, for 10 min in a flowing oxygen atmosphere.

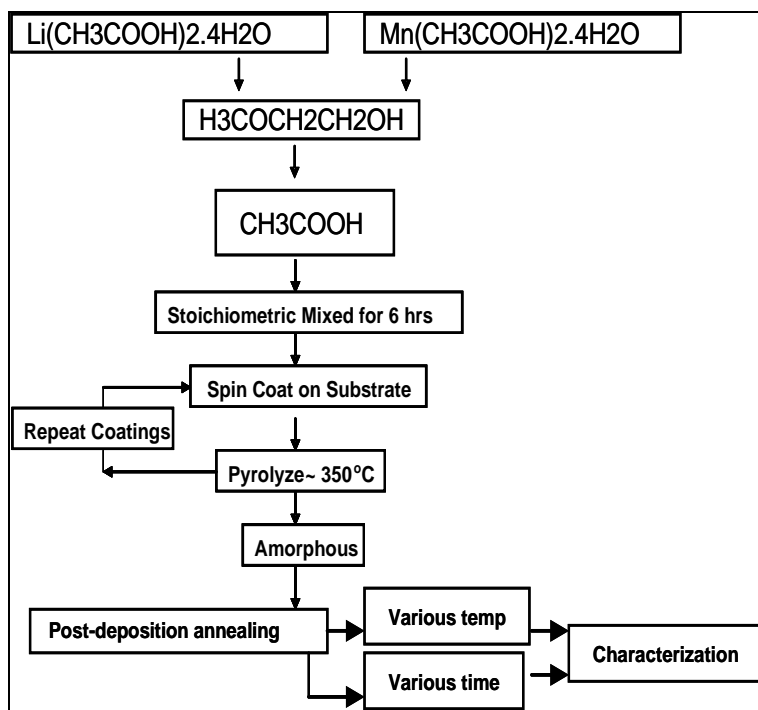


Figure 1. MOSD processing scheme of  $\text{LiMn}_2\text{O}_4$ .



## **2.3 Characterization**

### **2.3.1 GAXRD**

The GAXRD data was obtained from a Bruker D5005 Powder Diffractometer, fitted with a thin film attachment and Goebel mirrors. To avoid overlapping contributions from the substrate diffraction intensity, which may dominate the contributions from the thin film diffraction peaks, the detector scan parameters were used at the angle of 3–10° to ensure the true film properties were observed. The power was set at 40 kV and 40 mA and the detector scan parameters were from 15 to 65°. A step size of 0.002° two theta was used with a dwell time of 1 s per step.

### **2.3.2 AFM**

The surface morphology of the films was examined by a Digital Instrument's Dimension 3100 AFM using tapping mode with amplitude modulation. Tapping mode is a common imaging technique and is well suited for topographical imaging of surfaces, with vertical resolution ranging from one micron down to sub nanometer scales. Tapping mode involves scanning an AFM tip attached to the end of an oscillating cantilever across the thin film surface. The amplitude of oscillation ranges from 20 nm to 100 nm, with the frequency near the resonant peak of the cantilever. The tip lightly taps the films surface, altering the oscillatory motion as the scanner moves across the surface. A surface is imaged by adjusting the vertical position of the scanner to maintain a constant root mean square signal of oscillation. The oscillation is measured by a laser positioned by the user to reflect signal into a photodiode detector. This technique is better suited for these films versus contact mode since it allows reproducibility without scratching and scrapping the film surface. The scan area for these films was 1 x 1 micron. Both amplitude and height data were collected. The amplitude data yielded the 2D view to obtain surface roughness.

### **2.3.3 SEM**

SEM was carried out using a Hitachi S-4700 Field Emission SEM (FESEM) in high resolution mode. The sample thickness was obtained by imaging a freshly cleaved cross section at 90° and comparing with the calibrated instrument scale bar. Samples with Si substrates were imaged at 10 kV while those with sapphire or MgO substrates were imaged at 2 kV.

### **2.3.4 Electrochemical Measurements**

Measurements of electrochemical properties were performed in a coin cell configuration. For this test, thin films solution were directly deposited on a 10 x 10 mm stainless steel mesh disk coin cell with a layer of acetylene black carbon to ensure electrical conductivity throughout the film (11). The 10 layers of coated film were placed into 2-electrode coin cells with a lithium foil counter electrode and Celgard polypropylene separators. The electrolyte consisted of 1.0 M LiPF<sub>6</sub> in 30% ethylene carbonate/70% ethyl methyl carbonate. Electrochemical capacity was measured on a Maccor 4000 battery test system at a constant current for up to 25 cycles. The cells were run at  $9.0 \times 10^{-5}$  A, over the first two cycles during formation of the solid electrolyte

inter-phase (SEI). The remaining cycles were run at  $3 \times 10^{-4}$  A, approximately C/3. It's currently a challenge to adhere the acetylene black carbon on the mesh screen, although films were deposited enough to for mechanical testing; however, such experiments will be further discussed in the future findings.

### 3. Results and Discussion

Figures 2 and 3 show the XRD patterns of the  $\text{LiMn}_2\text{O}_4$  thin films as a function of annealing temperature and number of coats, respectively. The absence of diffraction peaks in the XRD patterns for films annealed up to 400 °C indicated that the films were likely amorphous. It was possible to obtain a well-crystallized phase with sharp (x,y,z) peaks and a minimal full width at half maximum (FWHM) at an annealing temperature of 700 °C with no evidence of secondary phases. As the annealing temperature was increased, the  $\text{LiMn}_2\text{O}_4$  peak intensity increased, the FWHM decreased, and grain size reduces due to the reduction in FWHM. These peaks are an indication of enhanced crystallinity. The XRD patterns show for films with 2 layers and 4 layers, shown in figure 3, shows weaker peaks intensity but at 6, 8, and 10 layers XRD confirmed crystallinity of the films containing 6 layers or more. The surface morphology of the films appeared smooth in AFM imaging, as shown in figure 4, with no cracks or defects. AFM and FESEM do show large whisker formation in the plane of the film though.

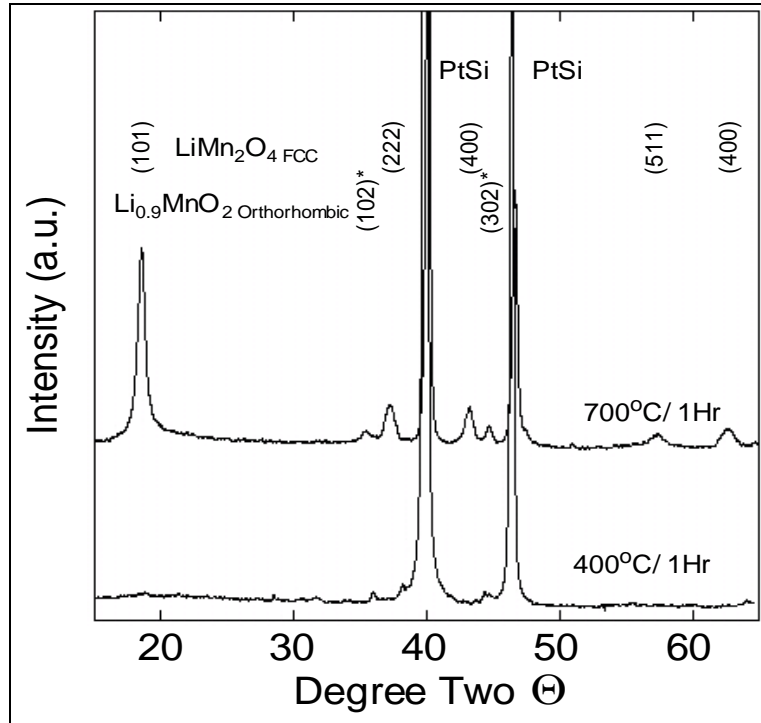


Figure 2. XRD patterns of the as-deposited  $\text{LiMn}_2\text{O}_4$  thin films on platinum silicon substrates at different annealing temperature (a) 400 °C; (b) 700 °C.

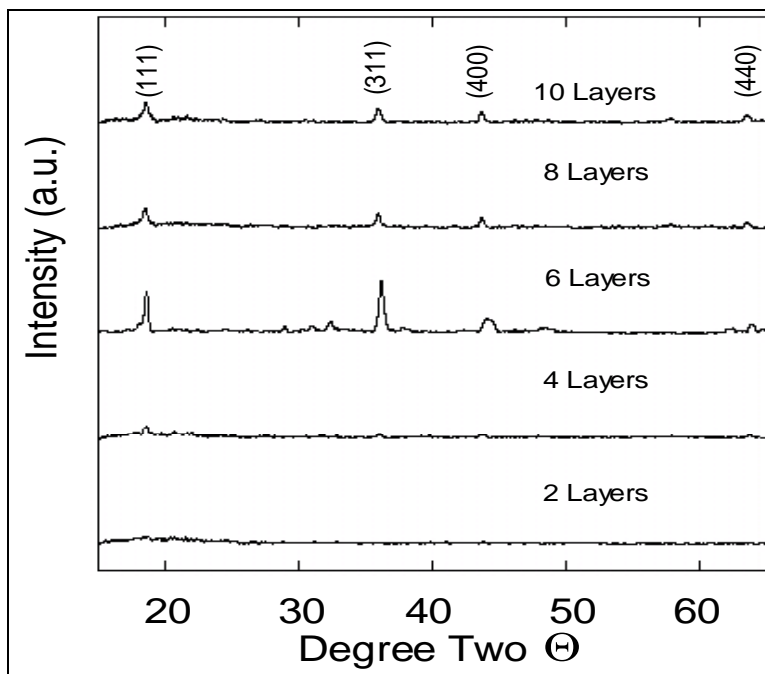


Figure 3. XRD patterns of the annealed  $\text{LiMn}_2\text{O}_4$  thin films on platinum silicon substrates at 750 °C at various layers showing at 6 layers and above crystallinity were able to be obtained.

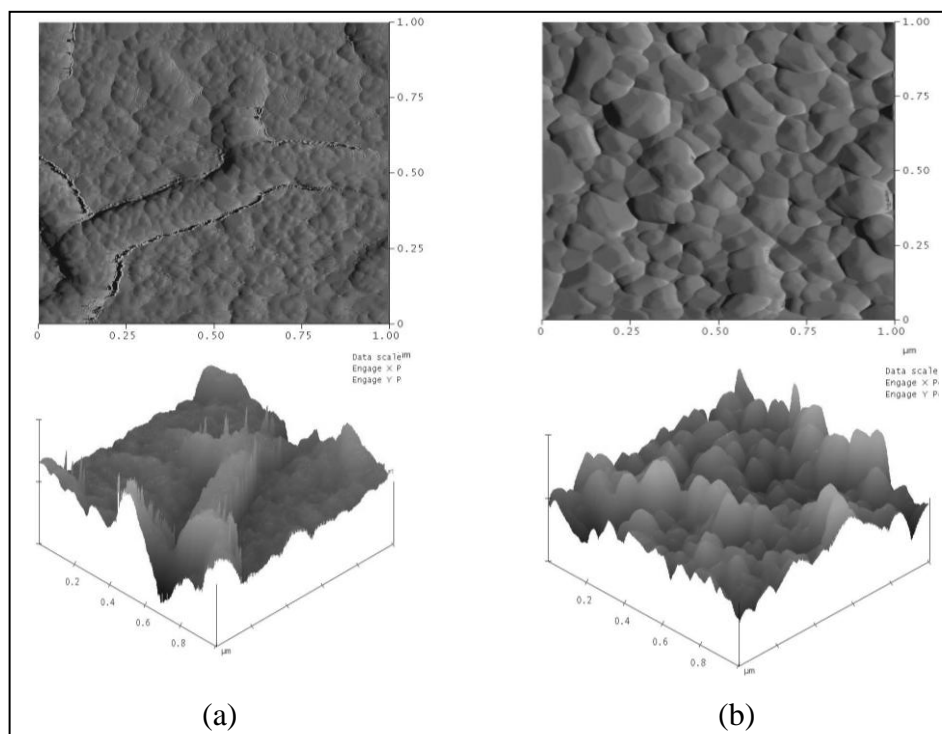


Figure 4. Atomic focus microscope shows the variation of the surface roughness and morphology with the annealing temperature (a) At 400 °C, the deposits exhibits earthworm-like morphology and (b) At 750 °C deposit exhibits dense and well-defined grains and earthworm-like vanished.

The films exhibited a dense microstructure and fine grain size. The average surface roughness was found to increase with a rise in annealing temperature with average surface roughness value of 40 nm at 750 °C as shown in figure 4. There was no appreciable effect of the annealing temperature on the microstructure of amorphous  $\text{LiMn}_2\text{O}_4$  thin films, while crystalline films showed an increase in grain size with increasing annealing temperature which is consistent with the XRD data. Larger grain sizes are expected with increasing annealing temperature because of amorphous to crystalline phase transformation and increase in surface mobility, thus allowing the films to decrease their total energy and grain boundary area by growing larger grains.

Figure 5 shows the variation of the surface roughness and morphology with the annealing temperature. At 400 °C, the films exhibited a worm-like morphology around 2.0–3.0 micron in length and 0.2 microns in width, with a gel-like appearance. The formation of a layer of under-composed organic components coating the spinel particles could be the origin of this uncharacteristic morphology. This hypothesis is consistent with the amorphous nature of the deposit as revealed by the XRD and AFM data. As the films are annealed, the worm-like shape gradually vanished, and at 750 °C the deposit surface is consisted of uniform polyhedral submicron grains. Above 750 °C, the particles developed a polyhedral morphology with distinct edges and features typical of the spinel-type structure and ranging in size from 0.2 to 0.6 microns. This observation is in agreement with other reports (10) and supported by the improved crystallinity (i.e., reduced FWHM) revealed by the XRD data.

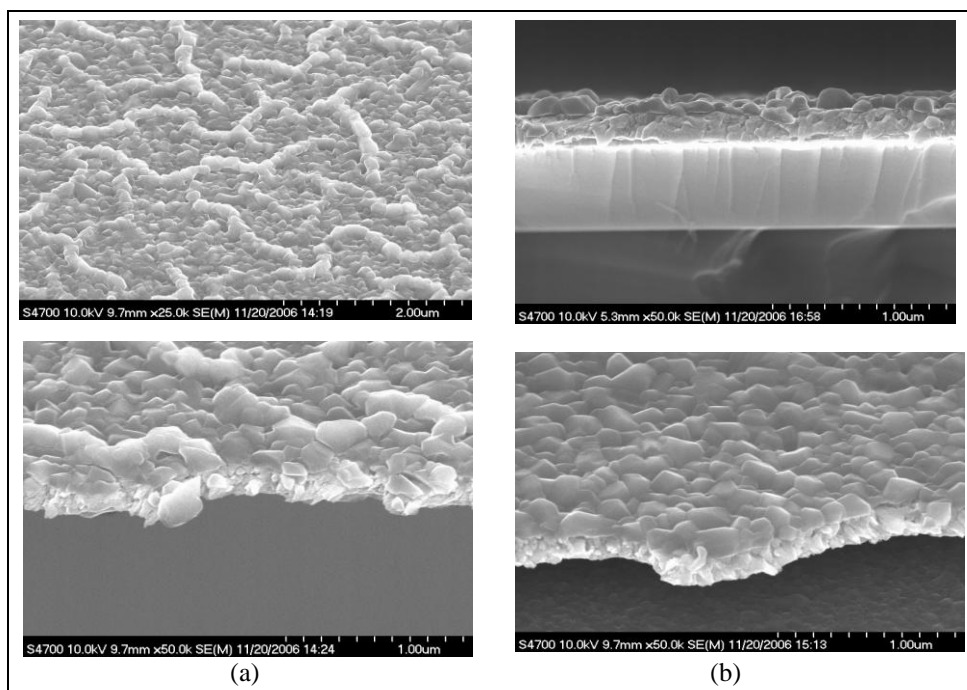


Figure 5. SEM and cross sectional of  $\text{LiMn}_2\text{O}_4$  thin films on platinum silicon substrates at different annealing temperature (a) 400 °C and 45 degree cross section (b) 750 °C and 45 degree cross section.

Figure 6a illustrates electrochemical behavior that was measured for one of the films. Due to the high bulk resistivity of  $\text{LiMn}_2\text{O}_4$ , the capacity is low and was difficult to obtain suitable measurements for many of the other samples. The drop in capacity over the first few cycles corresponds to interfacial resistances that are typically attributed to SEI formation. This initial capacity fade was found to be about 20% for these materials over the first 3 cycles followed by a flat region of little variation in which the capacity is reversible. The data shows a relatively low capacity, referred to as the reversible capacity that requires further investigation in the future to confirm the results. Figure 6b shows charges of  $\text{LiMn}_2\text{O}_4$  peaks after 2 hours and remains constant and stable after 35 hours. This data shows the charging process was located at potentials of about 4.00 and 4.18 volts. Variation in the potential calculations was due to the imprecise weight obtained and we were unable to get an exact measure of specific capacity ( $\text{mAh/g}$ ). By integrating with a stainless steel structural mesh wire to create a strong composite,  $\text{LiMn}_2\text{O}_4$  cathode thin films may be used in a structural composite battery.

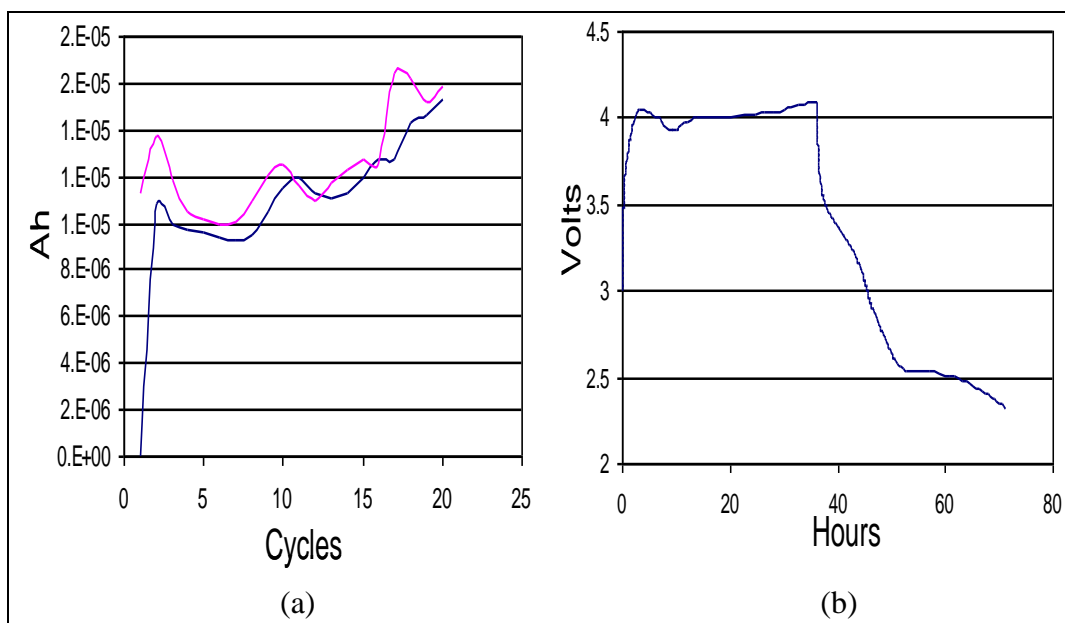


Figure 6. (a) Charge and discharge data curves of 20 cycles illustrate electrochemical behavior of the 6 layers film annealed at 750C. (b) Voltage profile over 60 hours of  $\text{LiMn}_2\text{O}_4$  films versus time.

## 4. Conclusion

Thin films were grown on various substrates and at various synthesis conditions using a solution spin coat growth technique. Spin-coating methodology is a useful tool for preparing homogeneous thin film of  $\text{LiMn}_2\text{O}_4$ . The morphology, structural and electrochemical analyses were performed on all of these films. The films annealed at 750 °C or above are homogenous and possessed good crystallization, morphology, micron-scale particle size, and uniform grain

size distribution. The electrochemical studies show that the films annealed at 750 °C or above were able to be cycled and exhibited measureable specific capacity which while not ideal indicate that with optimization, this is a promising technological solution to the structural issue. New materials or processing techniques will need to be employed to reduce the bulk resistivity of the materials; our results suggest that the processes described here could be used to develop cathodes that enable structural behavior.

---

## 5. References

---

1. South, J.; Carter, R. H.; Snyder, J. F.; Wetzel, E. D. 130, MRS Paper, 2003.
2. Scrosati, B.; Croce, F.; Panero, S. *J. Power Sources* **2001**, *100* (1–2), 93–100.
3. South, J. T.; Carter, R. H.; Snyder, J. F.; Hilton, C. D.; O'Brien, D. J.; Wetzel, E. D. *Proceedings of the 2004 MRS Fall Conference*, Boston, MA, 851, 2004.
4. Snyder, J. F.; Carter, R. H.; Wong, E. L.; Nguyen, P. A.; Xu, K.; Ngo, E. H.; Wetzel, E. D. *SAMPE Fall Technical Conference Proceedings 2006*, Dallas, TX, 2006.
5. Snyder, J. F.; Carter, R. H.; Wong, E. L.; Nguyen, P. A.; Xu, K.; Ngo, E. H.; Wetzel, E. D. *Proceedings of the 25th Army Science Conference*, 2006.
6. Mohamedi, M.; Takahashi, D.; Itoh, T.; Uchida, I. *Electrochim. Acta* **2002**, *47*, 3483.
7. Tang, S. B.; Lai, M. O.; Lu, L.; Tripathy, S. *Journal of Solid State Chemistry* **2006**, *179*, 3831–3838.
8. Joshi, P. C.; Cole, M. W. *Physics Letters* **July 2000**, *77* (2, 10).
9. Arrebola, José C.; Caballero, A´lvaro; Herna´n, Lourdes; Melero, Montserrat; Morales, Juli´an; Castell´on, Enrique R. *Journal of Power Sources* **2006**, *162*, 606–613.
10. Arrebola, José C.; Caballero, A´lvaro; Herna´n, Lourdes; Melero, Montserrat; Morales, Juli´an; Castell´on, Enrique R. *Journal of Power Sources* **2006**, *162*, 606–613.
11. Nazri; Pistoia, G. *Lithium Batteries Science and Technology*; Boston, Kluwer Academic Publishers, 2004, pp. 99–102, 347–350.

---

## List of Symbols, Abbreviations, and Acronyms

---

AFM	atomic force microscopy
$\text{CH}_3\text{COOH}$	acetic acid
FESEM	Field Emission SEM
FWHM	full width at half maximum
GAXRD	glancing angle X-ray diffraction
$\text{H}_3\text{COCH}_2\text{CH}_2\text{OH}$	2-methoxyethanol
$\text{LiMn}_2\text{O}_4$	lithium manganese oxide
$\text{Mn}(\text{CH}_3\text{COOH})_2 \cdot 4\text{H}_2\text{O}$	manganese acetate
MOSD	metal organic solution deposition
Pt-Si	platinum coated silicon substrates
Rpm	revolutions per minute
SEI	solid electrolyte inter-phase
SEM	scanning electron microscopy
UV	ultra violet



NO. OF COPIES	ORGANIZATION
1	ADMNSTR DEFNS TECHL INFO CTR ATTN DTIC OCP 8725 JOHN J KINGMAN RD STE 0944 FT BELVOIR VA 22060-6218
1 CD	OFC OF THE SECY OF DEFNS ATTN ODDRE (R&AT) THE PENTAGON WASHINGTON DC 20301-3080
1	US ARMY RSRCH DEV AND ENGRG CMND ARMAMENT RSRCH DEV & ENGRG CTR ARMAMENT ENGRG & TECHN LGY CTR ATTN AMSRD AAR AEF T J MATTS BLDG 305 ABERDEEN PROVING GROUND MD 21005-5001
1	US ARMY INFO SYS ENGRG CMND ATTN AMSEL IE TD A RIVERA FT HUACHUCA AZ 85613-5300
1	COMMANDER US ARMY RDECOM ATTN AMSRD AMR W C MCCORKLE 5400 FOWLER RD REDSTONE ARSENAL AL 35898-5000
1	US GOVERNMENT PRINT OFF DEPOSITORY RECEIVING SECTION ATTN MAIL STOP IDAD J TATE 732 NORTH CAPITOL ST NW WASHINGTON DC 20402
1	US ARMY RSRCH LAB ATTN RDRL WMM E C HUBBARD BLDG 4600 ABERDEEN PROVING GROUND MD 21005-5066
5	US ARMY RSRCH LAB ATTN RDRL WMM D R CARTER ATTN RDRL WMM E E NGO ATTN RDRL WMM E S GARRETT HIRSCH ATTN RDRL WMM G J SNYDER ATTN RDRL SED C C XU BLDG 4600 ABERDEEN PROVING GROUND MD 21005
3	US ARMY RSRCH LAB ATTN IMNE ALC HRR MAIL & RECORDS MGMT ATTN RDRL CIO LL TECHL LIB ATTN RDRL CIO MT TECHL PUB ADELPHI MD 20783-1197

INTENTIONALLY LEFT BLANK.